Electronic Structure of Layered MB_2C Rare-Earth Borocarbide Compounds

Fabrice Wiitkar,[†] Samia Kahlal,[†] Jean-François Halet,*[,†] Jean-Yves Saillard,*[,†] Josef Bauer,[‡] and Peter Rogl[§]

Contribution from the Laboratoire de Chimie du Solide et Inorganique Moléculaire, URA CNRS 1495, Université de Rennes I, 35042 Rennes, France, Laboratoire de Chimie du Solide et Inorganique Moléculaire, URA CNRS 1495, Institut National des Sciences Appliquées, 35043 Rennes, France, and Institut für Physikalische Chemie, Universität Wien, Währingerstrasse 42, A-1090 Wien, Austria

Received May 24, 1993. Revised Manuscript Received August 30, 1993[⊕]

Abstract: The electronic structure and bonding properties of the layered borocarbide compounds with the ThB_2C, α-UB_2C, and YB_2C structures are analyzed and compared by means of extended Hückel tight-binding calculations. These materials contain alternatively metallic and boron–carbon sheets. The results show that an ionic picture between the metallic and the boron–carbon sublattices is a good starting point to explain the arrangement observed in the different nonmetal networks. Thus, a formal charge of 4– per B_2C unit accounts for the structure of the B–C net in ThB_2C and α-UB_2C, whereas a formal charge of 3– must be attributed to the one in YB_2C. An alternative B_2C two-dimensional arrangement is proposed for the charge of 4– per B_2C. The semimetallic nature observed for all the anionic two-dimensional boron–carbon layers is discussed. In the three-dimensional materials, the metal–nonmetal bonding occurs primarily through electron donation from the anionic sublattice toward the metallic elements. Metallic behavior is expected for all the materials.

One of the most striking features of the solid-state rare-earth[1] borocarbide materials is their particularly rich and unique structural chemistry. As shown in Table 1, these ternary compounds of general formula $M_xB_yC_z$ can be classified in three different families, depending upon the way the boron and carbon atoms are linked together throughout the whole crystal. It turns out that the dimensionality of the boron carbon networks encountered in the solid materials can simply be associated with the averaged valence electron count per main group atom (VEC). This VEC is obtained assuming a simple ionic bonding scheme between the metal atoms and the B–C net, in which the metal is fully oxidized (usually M^{3+}, sometimes M^{4+} as in the case of Ce, Th, or U), in the following way:

$$\mathrm{VEC} = (nx + 3y + 4z)/(y + z)$$

with $n = 3$ or 4.

In the first class of compounds listed in Table 1, the main group atoms form infinite, planar, two-dimensional (2-D) layers, which alternate with 2-D sheets of metal atoms. They are characterized by a VEC comprised between 4.1 and 4.7. The compounds having a VEC around 5.0 belong to the second group and exhibit infinite, planar one-dimensional branched zigzag chains of light atoms embedded in a metallic lattice. Finally, in the third family, the boron and carbon atoms agglutinate to form finite chains which are more or less linear and which run into metallic channels. Chains made up from 2 to 13 atoms have been observed so far. Their VEC value spreads over the range 4.9–5.7. Although the VEC provides only a rough estimation of the electron-richness of the boron and carbon sublattice, it shows clearly the relationship which exists between the atom connectivity, i.e., the dimensionality of the B–C network, and the electron count. Adding electrons results in the occupation of antibonding orbitals and consequently leads to some bond breaking. Therefore, the larger the VEC, the lower the connectivity between the main group atoms. Note, however, that there is not a clear cut but a continuum in the VEC variation when going from one class to another.

Table 1. Three Different Families of Rare-Earth Borocarbides[e]

structural type		VEC[a]	B–C network	B/C	ref
		Two-Dimensional Networks			
LaB_2C_4	Ce, Ho, Er	4.17	$^2_\infty$-(2B4C)	0.5	2
LaB_2C_2	Y to Lu	4.25	$^2_\infty$-(2B2C)·(4B4C)	1.0	3
ScB_2C_2		4.25	$^2_\infty$-(2B3C)·(4B3C)	1.0	4
Yb_2C	Sc, Tb to Lu	4.33	$^2_\infty$-(2B3C)·(5B2C)	2.0	5
ThB_2C	Ce, U(h.t.[b]), Np, Pu	4.33 (4.67)	$^2_\infty$-(6B)·(6B(3C))	2.0	6
UB_2C(l.t.[c])		4.33 (4.67)	$^2_\infty$-(6B(2C))	2.0	7
$Gd_2B_3C_2$		4.60	$^2_\infty$-(8B4C)	1.5	8
		Infinite Branched Chains			
YBC	Dy, Ho, Er	5.00	$^1_\infty$-[B_2C_2]	1.0	5a
ThBC		5.00	$^1_\infty$-[B_2C_2]	1.0	9
UBC	Np, Pu	5.00 (5.50)	$^1_\infty$-[B_2C_2]	1.0	10
$UB_{0.78}C_{1.22}$		5.11 (5.61)	$^1_\infty$-[B_2C_2]	0.64	11
$Th_3B_2C_3$		5.00[d] (5.50)[d]	[C]-$^1_\infty$-[B_2C_2]	0.66	12
		Finite Linear Chains			
$La_{15}B_{14}C_{19}$		4.94	[B_4C_7][B_5C_6]	0.74	13
$Ce_{10}B_9C_{12}$	La, Nd	5.00	[B_5C_8][B_4C_4]	0.75	14
$Ce_{10}B_8C_{10}$		5.22	[B_4C_4][B_3C_3]-[BC_2][C]	0.8	15
$La_{10}B_9C_6$		5.40		1.5	13
$U_5B_2C_7$	Ho	5.44		0.29	16
$La_5B_2C_6$	Ce, Ho	5.63	[BC_2][C_2]	0.33	17
Sc_2BC_2	Y	5.67	[BC_2]	0.5	18

[a] Averaged valence electron count per main group atom. [b] High temperature. [c] Low temperature. [d] Value assuming the formal topochemical separation: ThC + 2ThBC ≡ $Th_3B_2C_3$. [e] The VEC is calculated with $n = 3$. It is given in brackets for $n = 4$ (see text).

It is obvious that this empirical observation needs to be completed with detailed results obtained from quantum mechanical calculations. Up to now, only a few theoretical studies have been devoted to the rationalization of the structure of the rare earth borocarbides and related phases.[8,19–22] As part of a general theoretical understanding of the structure and properties

† Université de Rennes I.
‡ Institut National des Sciences Appliquées.
§ Institut für Physikalische Chemie.
⊕ Abstract published in *Advance ACS Abstracts*, December 15, 1993.
(1) Throughout this paper, the word "rare-earth" refers to the elements Sc, Y, lanthanides, and actinides.

0002-7863/94/1516-0251$04.50/0

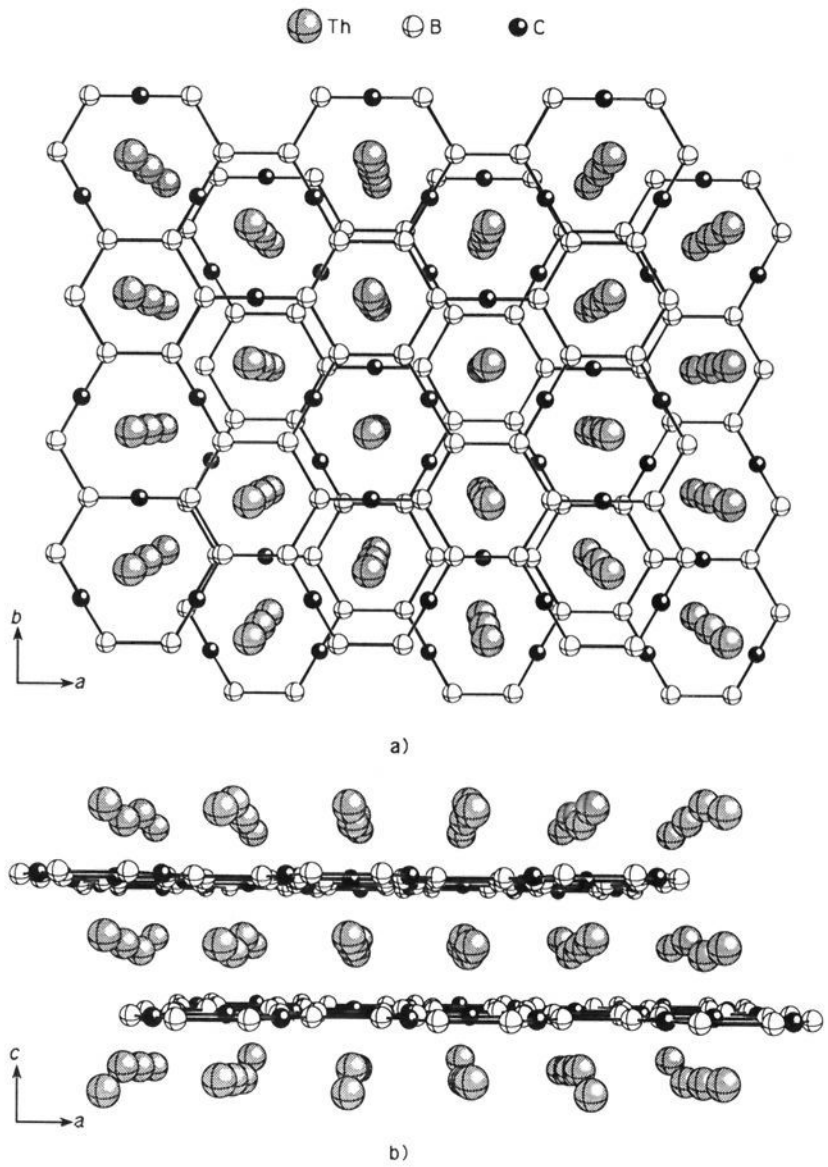

Figure 1. Crystal structure of ThB_2C.

of these compounds,[8,20] we undertake here the study of the rare-earth borocarbides of general formula MB_2C, using extended Hückel-type tight-binding calculations.[23] The computational details are gathered in the Appendix.

The Three Structural Types of MB_2C Phases

Three structural types have been characterized so far for the rare-earth borocarbides of MB_2C stoichiometry: ThB_2C, α-UB_2C, and YB_2C (see Table 1). The ThB_2C-type is encountered with M = Ce,[24] Th[6], U at high temperature, Np, and Pu.[25] ThB_2C crystallizes in the rhombohedral space group $R\bar{3}m$ with $Z = 9$.[6] A projection of the structure along the [001] and [010] directions is shown in Figure 1. The arrangement in ThB_2C can be described as an alternation of slightly puckered hexagonal layers of thorium and planar nets of main group atoms. The latter are made of fused nine-membered B_6C_3 rings and regular B_6 hexagons. The boron atoms are three-connected (to two boron and one carbon atoms) with valence angles equal to 120°. The carbon atoms are two-connected with valence angles equal to 180°. Thus, the building block of the 2-D net of nonmetals, shown in **1**, is made of a central sp carbon atom and two sp^2 terminal boron atoms. The B–C distance (1.49 Å) indicates some character of double bond, whereas the B–B distance (1.85 Å) suggests a bond order of one. Bonding seems also present between metal atoms as well as between metal and nonmetal atoms as shown by the measured interatomic separations.[6] Let us mention that a planar two-dimensional Fe_2C arrangement analogous to the B–C one present in ThB_2C has been recently reported in $Ho_2Fe_{17}C_{3-x}$.[26]

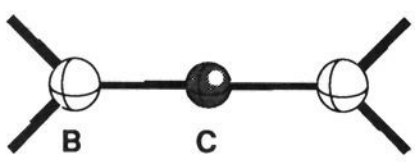

1

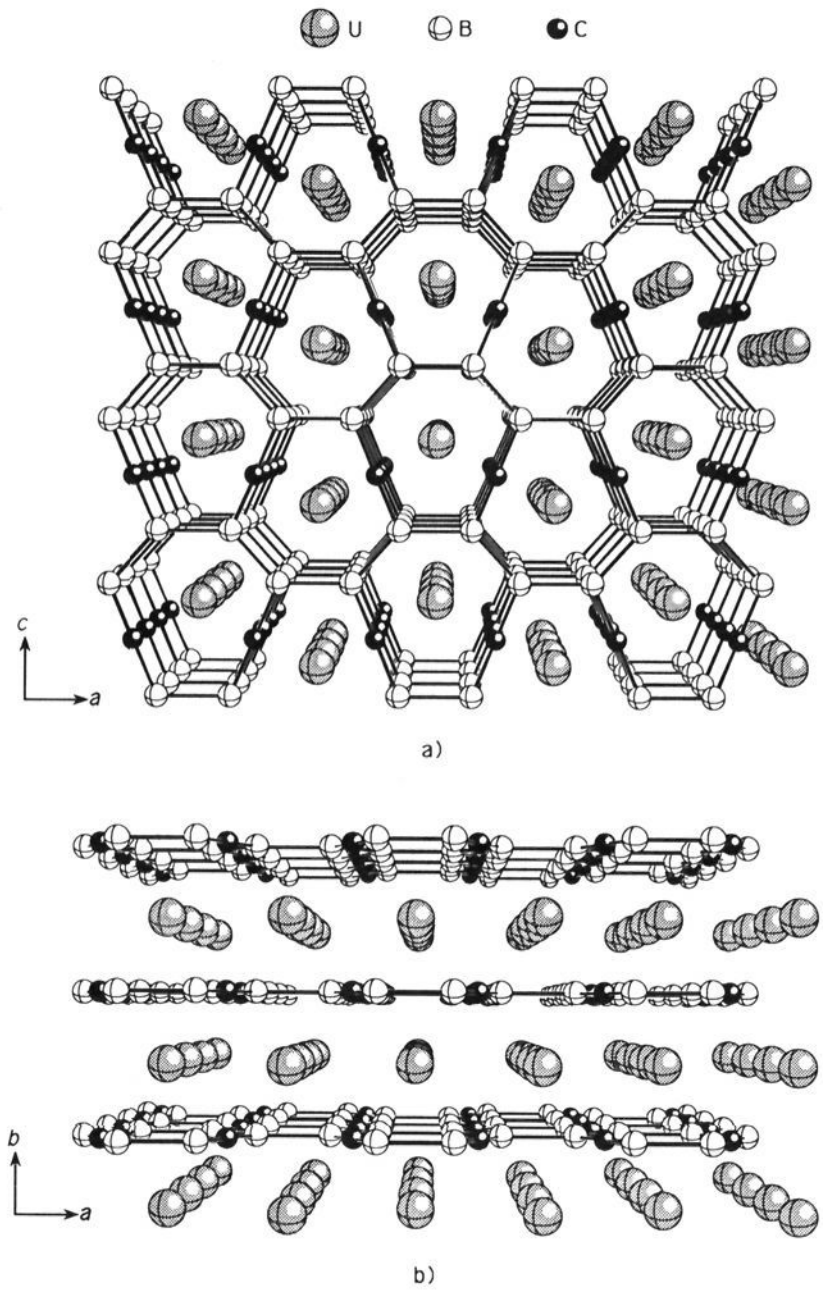

Figure 2. Crystal structure of α-UB_2C.

The α-UB_2C structural type (low-temperature modification) is orthorhombic and crystallizes in the space group *Pmma* with $Z = 2$.[7] A projection of the structure along the [010] and [001] directions is shown in Figure 2. In this structure, planar nonregular hexagonal layers of uranium atoms alternate with planar nets of boron and carbon atoms made of fused eight-membered B_6C_2 rings. The connectivity of the boron and carbon atoms is exactly the same as in ThB_2C. The valence angles around each boron atom (115°, 113°, 132°) indicate a distorted sp^2 hybridization, while the coordination of the carbon atom is perfectly linear, as in ThB_2C. Not only the connectivity between the atoms is similar in the two types of layers but also the B–C and B–B bond distances are similar (ca. 1.5 and 1.8 Å, respectively).[7] It results that the basic building block of the light-atom 2-D net of α-UB_2C is also **1**, as in ThB_2C. The similarities between the two compounds can be extended to the metal–metal (distorted hexagonal sheets) and the metal–light atom bonding (compare Figures 1 and 2). Indeed, in both compounds, the boron atoms occupy the centers of M_6 triangular prisms, while the carbon atoms occupy the centers of M_4 squares. The structural relationship existing between ThB_2C and α-UB_2C is exemplified by the fact that the high-temperature modification of UB_2C (β-phase) adopts the ThB_2C structural type.

Though it presents also planar sheets of metal atoms alternating with planar layers of nonmetal atoms, the structure of YB_2C is somehow different from that of ThB_2C or α-UB_2C (see Figure 3).[5] In this compound, which crystallizes in the tetragonal space group, $P4_2/mbc$ with $Z = 4$,[5] the metallic 2-D net is made of fused squares and triangles, while the main group 2-D net is made of four- and seven-membered fused rings. All the light atoms are tricoordinated, adopting a distorted sp^2 hybridization. Although they are not very accurate, the B–B bond distances (1.77–1.84 Å) suggest single bonds, while the B–C bond distances

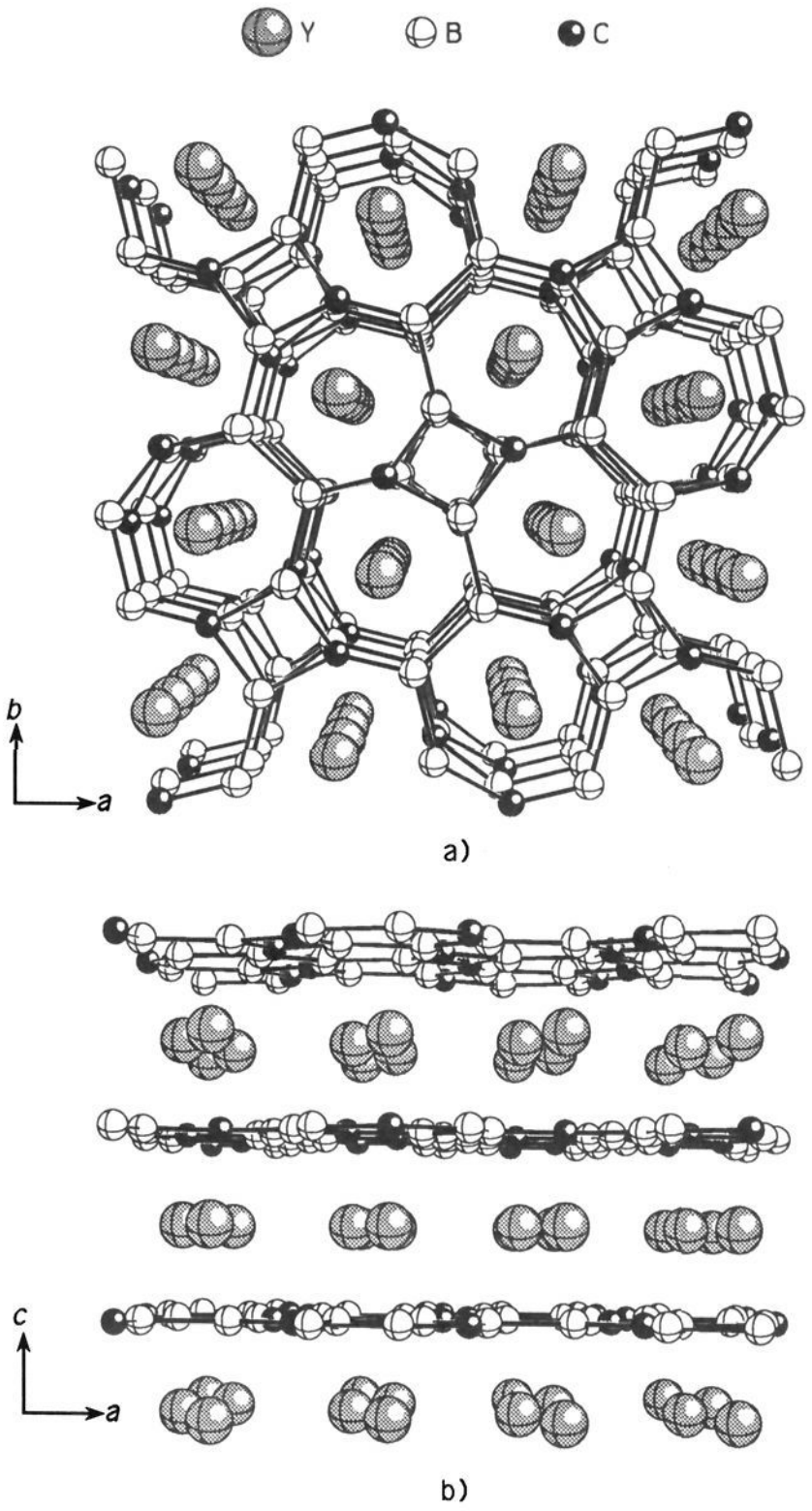

Figure 3. Crystal structure of YB_2C.

(1.54–1.69 Å) suggest some partial double bond character.[5] The arrangement between the metal and nonmetal atoms is also different in this phase. The metal sheets, distant of 3.72 Å from each other, stack along the *c*-axis in an eclipsed fashion in order to form large cubes and trigonal prisms, where are embedded B_2C_2 rhombuses and B atoms of the B–C net, respectively (see Figure 3).

Since the ThB_2C and α-UB_2C phases appear strongly related, let us discuss first the electronic structure of these two compounds together. The electronic structure of YB_2C will be analyzed and compared later.

Electronic Structure of ThB_2C and α-UB_2C

Following the approach used by Burdett *et al.* in their theoretical study of MB_2C_2 phases,[19] we shall first tackle the B–B and B–C bonding analysis within the framework of an ionic bonding scheme between the metal and the nonmetal sublattices. In a second step, we shall consider the orbital interactions between both sublattices.

(a) The 2-D Nets of Boron and Carbon. Assuming a pure ionic bonding mode between the metal atoms and the nonmetal 2-D nets, the first question which arises concerns the ionic charges. The most usual oxidation state for the rare-earth elements is 3+.[27] However, thorium makes an exception with an usual oxidation state of 4+ ($5f^06d^07s^0$).[27] In the case of uranium, both oxidation states of 3+ ($5f^36d^07s^0$) and 4+ ($5f^26d^07s^0$) are common.[27] In addition, since metal–metal bonding is present in the studied compounds, the possibility of a partly filled d-band, and consequently of an oxidation state lower than 3+ for the metal atoms, cannot be ruled out.

One can shed some light on the problem of the formal anionic charge of the $[BCB]^{n-}$ repeat unit (**1**) present in ThB_2C and α-UB_2C, by looking at the electronic structure of its simplest molecular analog, namely $[H_2BCBH_2]^{n-}$. Since the B–C separations in the building block **1** indicate some double bond character, a Lewis structure such as **2**, corresponding to $n = 2$, can be proposed. This would make the anionic molecule isoelectronic to allene (H_2CCCH_2), which is well-known to be a nonplanar molecule (D_{2d} symmetry).[28] As shown in Figure 4, which represents the extended Hückel–Walsh diagram and total electronic energy variation for the D_{2d} (nonplanar) $\rightarrow$ D_{2h} (planar) transformation of the model $[H_2BCBH_2]^{n-}$, the D_{2d} structure is preferred for $n = 2$, as for the isoelectronic allene analog. However, for $n = 4$ or 3, the D_{2d} arrangement is Jahn–Teller unstable, and the planar structure is favored. Therefore, these charges of 3– or 4– could account for the planar nature of the studied nonmetal layers. In the case of $n = 4$, the MO diagram is consistent with the Lewis formula shown in 3. The formal B–C bond order is 1.5, in good agreement with the observed bond distances measured in ThB_2C and α-UB_2C.[6,7]

If a charge of 4– (or possibly 3–) is assumed per B_2C, one understands now why the repeat unit **1** is planar. However, a new question arises: why is the carbon atom linearly coordinated, when the Lewis formula **3** suggests an sp^2-type hybridization for this atom? Compounds isoelectronic to the model $[H_2BCBH_2]^{4-}$, such as the allyl anion or SO_2, are bent.[28,29] We first checked that extended Hückel calculations reproduce correctly the strong

(2) Markovskii, L.; Vekshina, N. V.; Pron, G. F. *Zh. Prikl. Khim.* **1965**, *38*, 245.
(3) Bauer, J.; Bars, O. *Acta Crystallogr.* **1980**, *B36*, 1540.
(4) Smith, G. S.; Johnson, Q.; Nordine, P. C. *Acta Crystallogr.* **1965**, *19*, 668.
(5) (a) Bauer, J.; Nowotny, H. *Monatsh. Chemie* **1971**, *102*, 1129. (b) Bauer, J. *J. Less-Common Met.* **1982**, *87*, 45. (c) Bauer, J.; Gougeon, P., unpublished results.
(6) Rogl, P.; Fischer, P. *J. Solid State Chem.* **1989**, *78*, 294.
(7) Rogl, P.; Fischer, P. *J. Solid State Chem.* **1991**, *90*, 285.
(8) Rogl, P.; Bauer, J.; Wiitkar, F.; Halet, J.-F.; Saillard, J.-Y. *Inorg. Chem.* **1994**, in press.
(9) Rogl, P. *J. Nucl. Mater.* **1978**, *73*, 198.
(10) Toth, L.; Nowotny, H.; Benesovsky, F.; Rudy, E. *Monatsh. Chemie* **1961**, *92*, 794.
(11) Rogl, P.; Rupp, B.; Felner, I.; Fischer, P. *J. Solid State Chem.* **1993**, *104*, 377.
(12) Rogl, P. *J. Nucl. Mater.* **1979**, *79*, 154.
(13) Lahrech, M. Ph.D. Thesis, Université de Rennes I, Rennes, France, 1990.
(14) Bonhomme, F.; Gosselin, P.; Ansel, D.; Bauer, J., unpublished results.
(15) Bauer, J. *10th International Symposium on Boron, Borides and Related Compounds*, Albuquerque, New Mexico, 27–30 August 1990.
(16) Rogl, P.; Bauer, J.; Debuigne, J. *J. Nucl. Mater.* **1989**, *165*, 74.
(17) Bauer, J.; Bars, O. *J. Less-Common Met.* **1983**, *95*, 267.
(18) Bauer, J.; Potel, M.; Gougeon, P.; Padiou, J.; Noël, H. *Proc. of the IXth Int. Conf. on Solid Compounds of Transition Elements* (*Royal Soc. of Chem. Dalton Division*), Oxford: G-B, 4–8 July 1988.
(19) Burdett, J. K.; Canadell, E.; Hughbanks, T. *J. Am. Chem. Soc.* **1986**, *108*, 3971.
(20) Halet, J.-F.; Saillard, J.-Y.; Bauer, J. *J. Less-Common Met.* **1990**, *158*, 239.
(21) Switendick, A. C. *10th International Conference on Solid Compounds of Transition Elements*; Münster, RFA, 21–25 Mar 1991.
(22) Lohr, L. L. *Int. J. Quantum Chem.* **1991**, *25*, 121.
(23) (a) Hoffmann, R. *J. Chem. Phys.* **1963**, *39*, 1397. (b) Whangbo, M.-H.; Hoffmann, R.; Woodward, R. B. *Proc. R. Soc. Lond.* **1979**, *A366*, 23. (c) Whangbo, M.-H.; Hoffmann, R. *J. Am. Chem. Soc.* **1978**, *100*, 6093.
(24) Bauer, J.; Ansel, D.; Bonhomme, F.; Gosselin, P. *J. Less-Common Met.* **1990**, *157*, 109.
(25) Rogl, P. In *The Physics and Chemistry of Carbides, Nitrides and Borides*; Freer, R., Ed.; Kluwer Academic Publishers: Netherlands, 1990; p 269.
(26) Bocelli, G.; Calestani, G.; Leccabue, F.; Watts, B. E.; Ll. Sanchez, J. L. *Chem. Mater.* **1993**, *5*, 129. Note, however, that this alloy is better described as a metal carbide interstitial compound since the C atoms lie in Ho_2Fe_4 octahedra.
(27) See, for example: Greenwood, N. N.; Earnshaw, A. *Chemistry of the Elements*, Pergamon Press: Oxford, 1984.

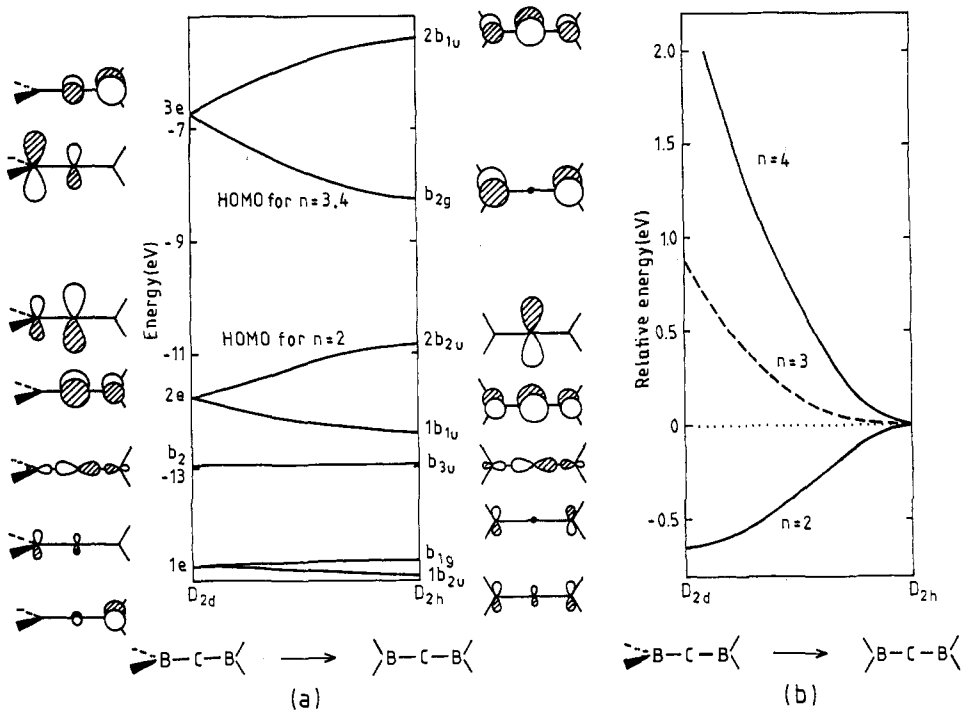

Figure 4. Extended Hückel–Walsh diagram (a) and total electronic energy variation for the D_{2d} (nonplanar) → D_{2h} (planar) transformation (b) of the model $[H_2BCBH_2]^{n-}$.

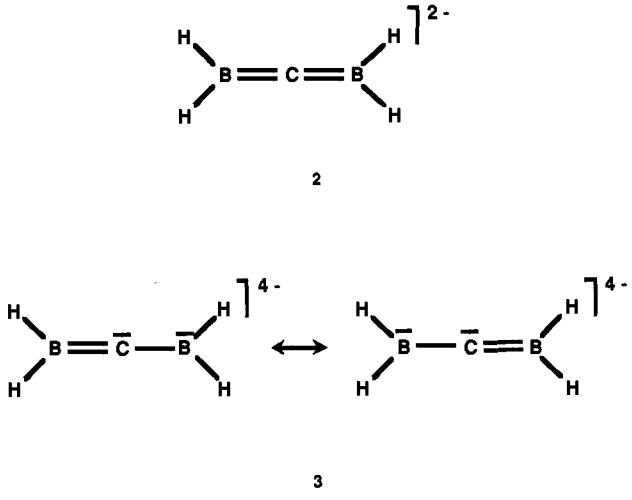

2

3

energy preference for the bent structure in the two latter species (by more than 2 eV). We calculated then the electronic energy variation with respect to the bending of the central carbon atom in the planar form of the models $[H_2BCBH_2]^{n-}$ (n = 3, 4) and $[H_2CCCH_2]^{2-}$. It is noteworthy to see in Figure 5, that the bent structure is found slightly preferred for the allenic dianion case, but the linear structure is favored for the isoelectronic model $[H_2BCBH_2]^{4-}$ and even for $[H_2BCBH_2]^{3-}$. The problem of the bending of triatomic systems is generally related to a second-order Jahn–Teller instability, which is the result of a three-orbital interaction pattern.[30] In the case of $[H_2CCCH_2]^{2-}$ or $[H_2BCBH_2]^{4-}$, this three-orbital system is shown in **4**. Upon bending, the symmetry is lowered, and the three orbitals are allowed to mix together. In the case of $[H_2CCCH_2]^{2-}$, the stabilizing mixing of the upper vacant antibonding orbital in the nonbonding HOMO predominates over the destabilizing mixing with the occupied

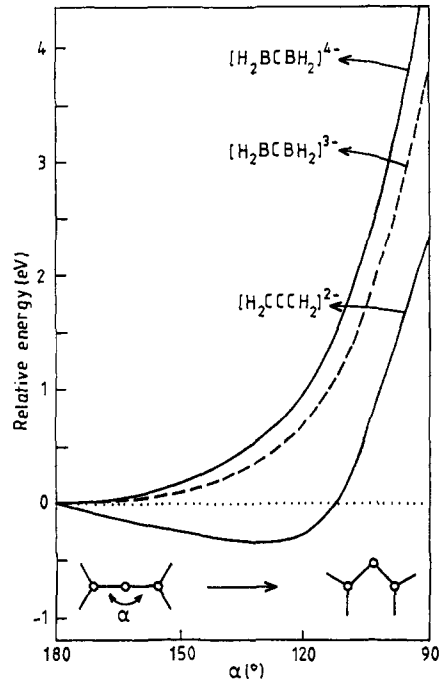

Figure 5. Electronic energy variation as function of the bending of the central carbon atom in the planar models $[H_2BCBH_2]^{n-}$ (n = 3, 4) and $[H_2CCCH_2]^{2-}$.

bonding orbital. The bent structure is consequently preferred since the HOMO is stabilized. Due to the more electropositive nature of boron compared to that of carbon,[31] the substitution in the linear structure of the two terminal carbon atoms by two B^- anions causes a destabilization of both the bonding and antibonding orbitals shown in **4**. The consequence is that this time the destabilizing mixing of the lowest orbital in the nonbonding HOMO predominates. This situation favors the linear structure, *i.e.*, an sp-type carbon atom.[32] The linear

(28) (a) Jorgensen, W. L.; Salem, L. *The Organic Chemist's Bood of Orbitals*, Academic Press: New York, 1973 and references therein. (b) See also: Liang, C.; Allen, L. C. *J. Am. Chem. Soc.* **1991**, *113*, 1873 and references therein.

(29) Wells, A. F. *Structural Inorganic Chemistry*, 5th ed.; Clarendon Press: Oxford, 1984.

(30) Albright, T. A.; Burdett, J. K.; Whangbo, M.-H. *Orbital Interaction in Chemistry*, Wiley Interscience: New York, 1985.

(31) Pauling, L. *The Nature of the Chemical Bond*; Cornell University Press: Ithaca, 1960.

(32) Note that in the case of SO_2, the electronegativity effect works in the other way, strongly favoring the bent structure.

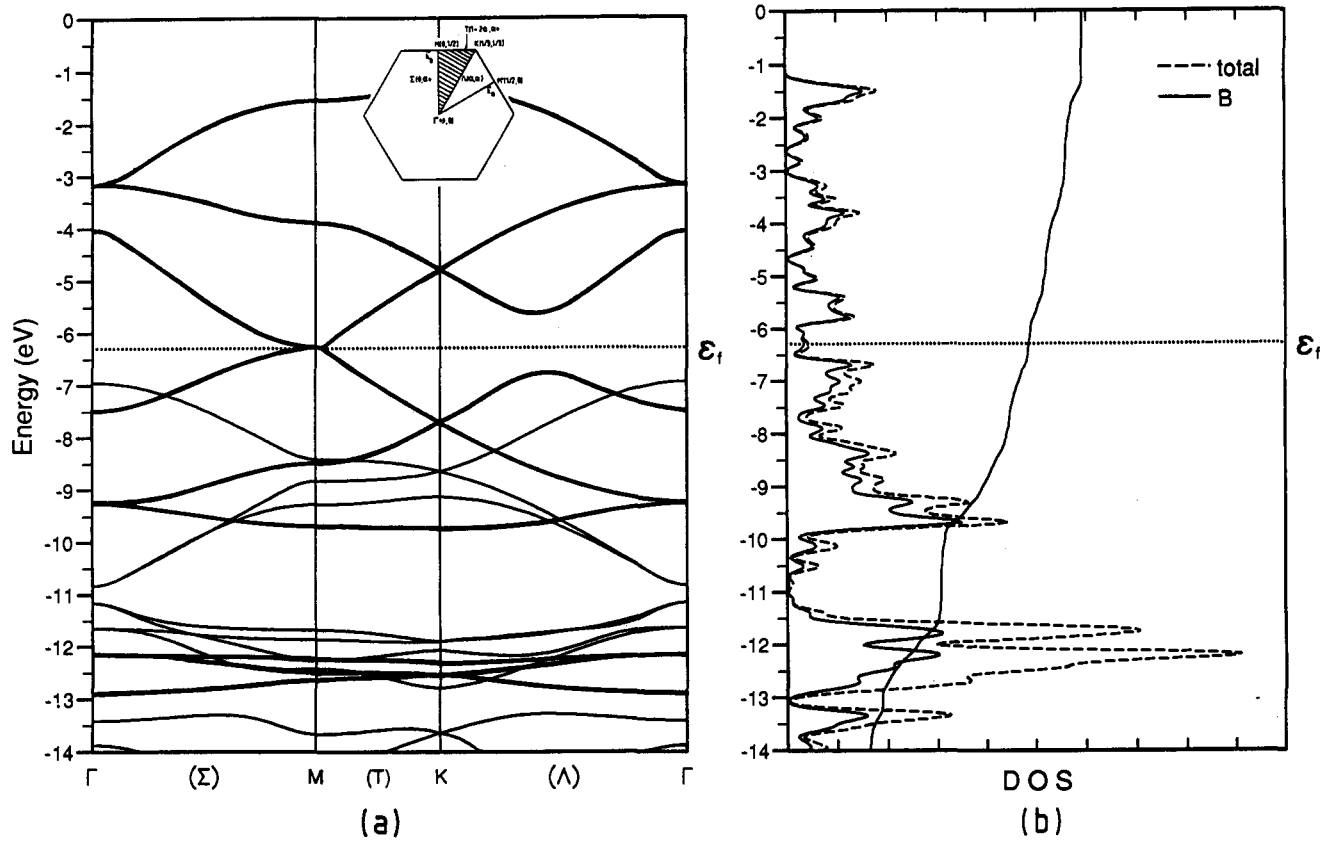

Figure 6. (a) Band structure and (b) total density of states (dashed line) and boron contribution (solid line) for the 2-D boron–carbon net encountered in ThB_2C. The Fermi level is indicated for a charge of 4– per B_2C unit. π-bands are in bold line.

preference for the $[H_2CBCH_2]^{4-}$ model or isoelectronic species respecting the same electronegativity difference between the central and the terminal atoms, has been confirmed by ab initio calculations using large basis sets and the Møller–Plesset perturbation expansion.[33]

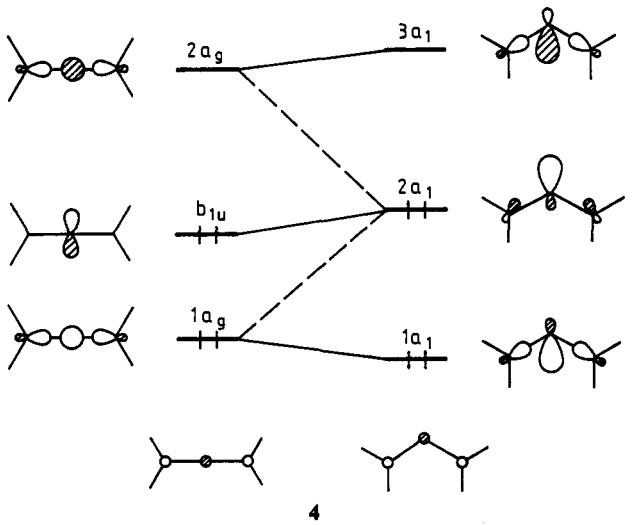

4

It results from the above analysis of the simple molecular model $[H_2BCBH_2]^{n-}$ that the adequate formal ionic charge for the building unit B_2C **1** is 4– (i.e., 14 valence electrons). Though the 3– charge (i.e., 13 valence electrons) would also account for the planar D_{2h} structure, its radical nature could induce some distortion of the 2-D layers. There is no experimental evidence for such a distortion. Moreover, note that whatever the temperature is we were unsuccessful in preparing compounds having the ThB_2C or α-UB_2C structure-type with trivalent elements such as La, Pr, Nd, or Sm. Therefore, the 3– formal charge per B_2C unit appears less probable. In order to check these preliminary conclusions, we have undertaken tight-binding calculations on the B_2C 2-D nets of ThB_2C and α-UB_2C.

(33) Frapper, G.; Halet, J.-F.; Saillard, J.-Y.; Volatron, F., to be published.

Table 2. Characteristics Computed with Different Electron Counts for the 2-D B_2C Layers

				overlap populations		atomic net charges		
EN[a]	net	RE[b]	ϵ_F[c]	B–B	B–C	B	C	π-electrons[d]
12	Th	0.0	−8.93	0.798	1.130	−0.16	−1.62	2.79
12	U	0.52	−8.90	0.815	1.082	−0.12	−1.76	2.71
12	Y	0.80	−8.32	1.003	0.821	−0.22	−1.55	3.00
12	**6**	0.06	−9.12	0.840	1.010	−0.07	−1.87	2.71
13	Th	0.0	−7.98	0.890	1.050	−0.54	−1.91	3.33
13	U	0.52	−8.12	0.914	0.996	−0.49	−2.03	3.26
13	Y	1.91	−6.41	1.043	0.754	−0.64	−1.72	4.00
13	**6**	−0.12	−8.22	0.943	0.929	−0.44	−2.12	3.29
14	Th	0.0	−6.29	0.983	0.859	−0.88	−2.23	4.00
14	U	0.06	−6.66	0.992	0.863	−0.86	−2.28	4.00
14	Y	3.66	−3.47	0.914	0.670	−1.08	−1.84	5.00
14	**6**	−0.82	−6.99	1.014	0.819	−0.83	−2.34	4.00

[a] Electron number per B_2C unit. [b] Relative energy per B_2C unit (eV) for a given electron count. [c] Fermi level (eV). [d] Per B_2C unit.

The band structure and density of states (DOS) of these 2-D organic nets are shown in Figures 6 and 7. The variation of the B–B and B–C overlap populations with respect to energy (COOP curves)[34] is represented in Figure 8 (a and b). One can see that the DOS and the COOP curves have similar shapes in both arrangements, indicating a close relationship between the electronic structure of the two boron–carbon nets. This is corroborated by the data gathered in Table 2, which give the population analysis, total electronic energies, and Fermi levels for several electron counts. Note that both nets are found almost isoenergetic for

(34) (a) Hughbanks, T.; Hoffmann, R. *J. Am. Chem. Soc.* **1983**, *105*, 3528. (b) Wijeyesekara, S. D.; Hoffmann, R. *Organometallics* **1984**, *3*, 949. (c) Kertesz, M.; Hoffmann, R. *J. Am. Chem. Soc.* **1984**, *106*, 3483.

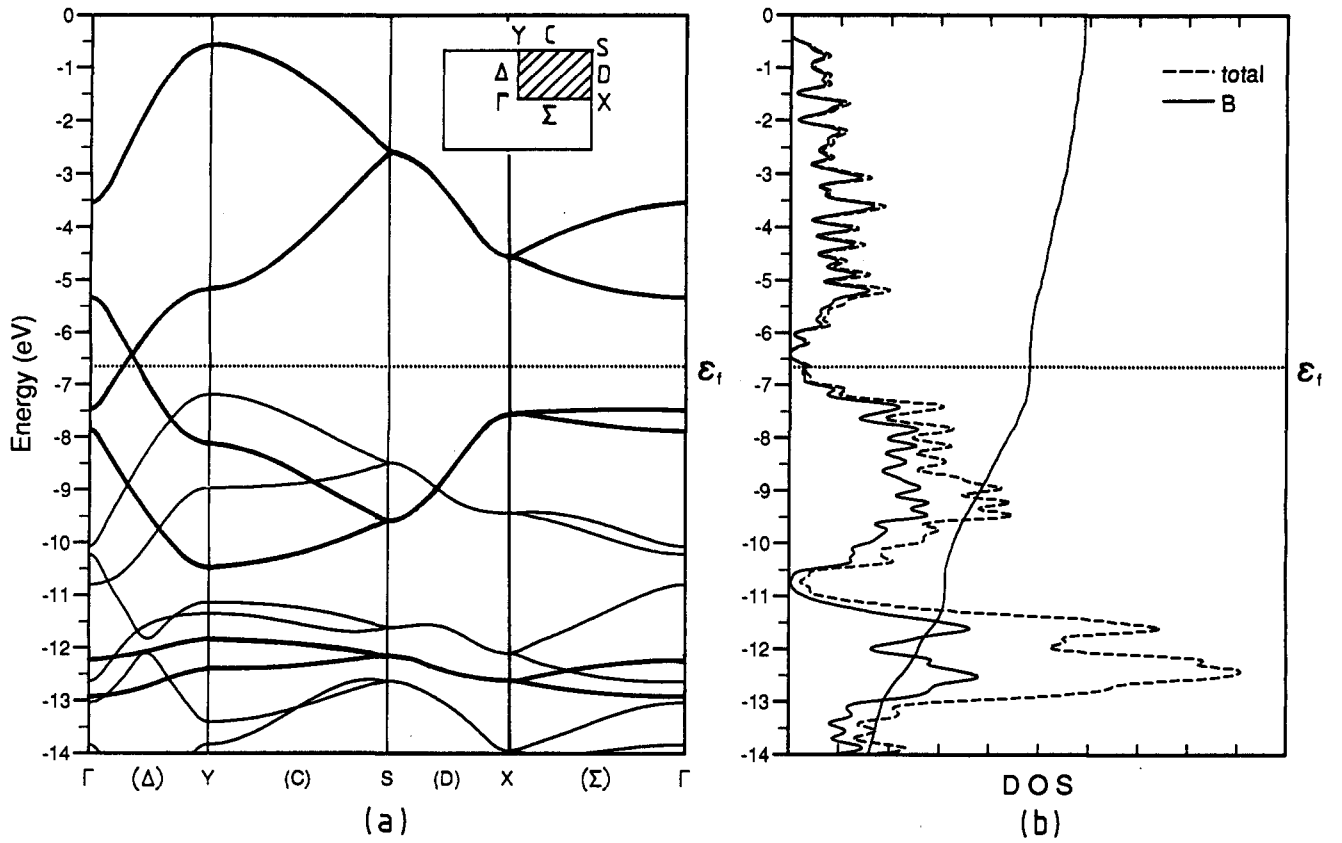

Figure 7. (a) Band structure and (b) total density of states (dashed line) and boron contribution (solid line) for the 2-D boron–carbon net encountered in α-UB_2C. The Fermi level is indicated for a charge of 4– per B_2C unit. π-bands are in bold line.

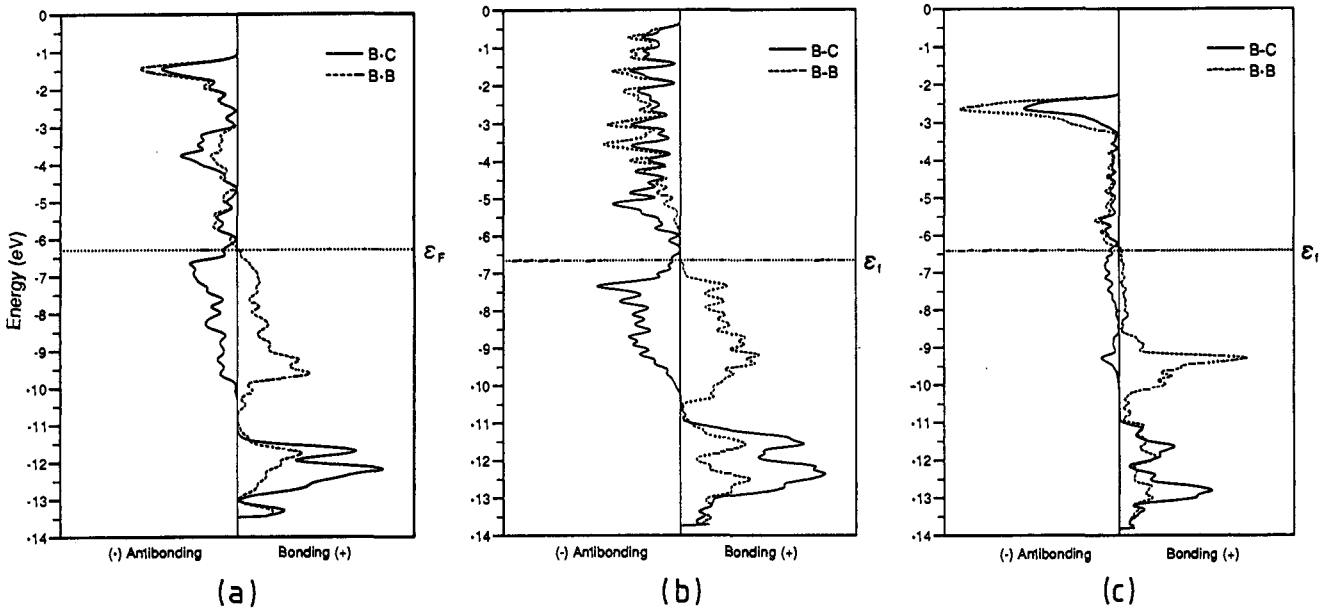

Figure 8. COOP curves for B–B and B–C contacts in the 2-D boron–carbon net of (a) ThB_2C, (b) UB_2C, and (c) YB_2C. The Fermi level is indicated for a charge of 4– per B_2C unit in (a) and (b), for a charge of 3– in (c).

any electron count. For $n = 4$, the overlap populations and band occupations (see Table 2, Figures 6a and 7a) are consistent with the Lewis structure depicted in **3** (four π-electrons). For this electron count, the B–B COOP curves change their bonding character into an antibonding one, almost exactly at the Fermi level, while the B–C COOP curves are already largely antibonding below the Fermi level. This is a situation often encountered in the main group sublattices of rare-earth borocarbides.[8,19,20,35] This typical feature is analyzed further. The band structure of the 2-D net of the thorium derivative shows an accidental degeneracy at the M point (see Figure 6a). Such a situation would confer a semimetallic behavior to a hypothetical isolated $[B_2C]^{4-}$ net. Comparatively, the band structure and DOS curve of the 2-D net of the uranium derivative (see Figure 7) show also a small number of states around the Fermi level for $n = 4$. Again, this is a semimetallic situation-type for the considered hypothetical $[B_2C]^{4-}$ net. This point will be discussed later.

(b) The Full ThB_2C and α-UB_2C Structures. Let us discuss

(35) This phenomenon is also noticed in rare earth borocarbide compounds of MBC formula: Wiitkar, F.; Kahlal, S.; Halet, J.-F.; Saillard, J.-Y.; Bauer, J.; Rogl, P., to be published.

(36) Hoffmann, R.; Janiak, C.; Kollmar, C. *Macromolecules* **1991**, *24*, 3725.

(37) Ramirez, R.; Böhm, M. C. *Int. J. Quantum Chem.* **1986**, *30*, 391.

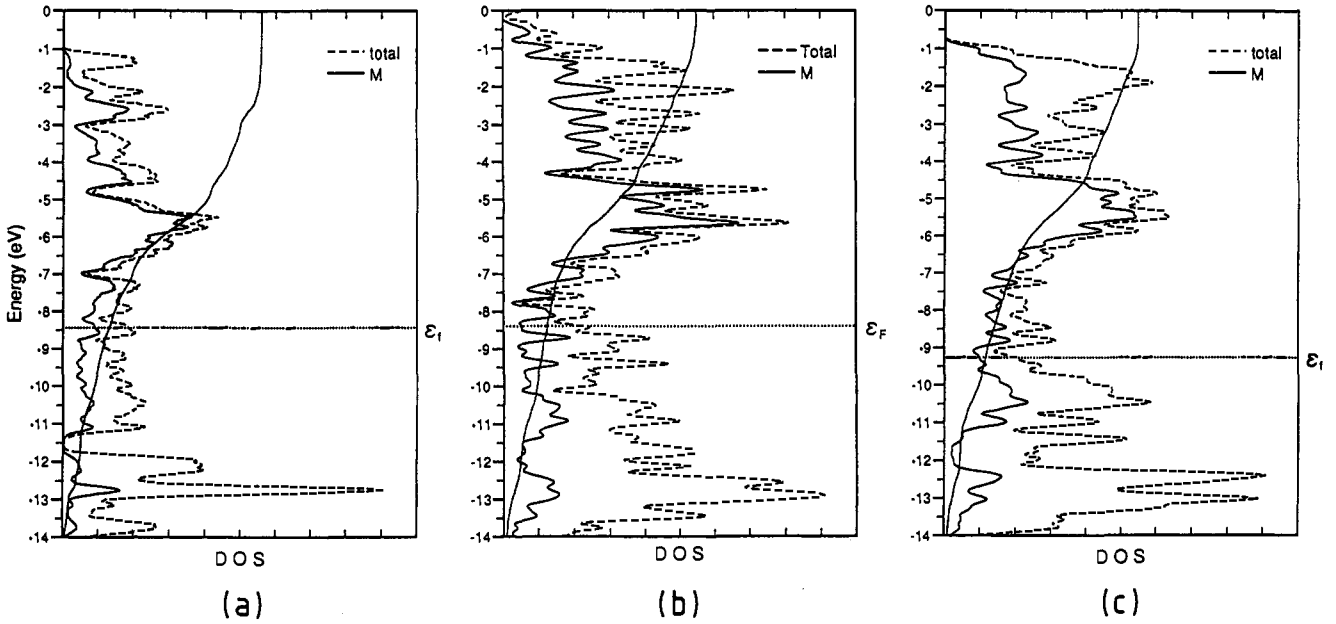

Figure 9. Total DOS (dashed line) and metal contribution (solid line) of (a) ThB_2C, (b) α-UB_2C, and (c) YB_2C. The Fermi level is indicated for a metal with four valence electrons in (a) and (b) and with three in (c).

now the importance of the interactions between the metallic and light-atom layers. Tight-binding calculations using the extended Hückel formalism have been performed on both ThB_2C and α-UB_2C structures. For the sake of comparison, the same set of atomic parameters for the metals has been used (see Appendix). The total DOS curves and their metallic contribution of the two structures are illustrated in Figure 9 (a and b). Overlap populations, total electronic energies, and Fermi levels for two electron counts (corresponding to trivalent and tetravalent metal atoms, respectively) are given in Table 3. As for the B_2C 2-D nets, results are comparable for both three-dimensional materials ThB_2C and α-UB_2C, reflecting their relationship. Despite the lamellar nature of the species, an isotropic conducting behavior is expected for the two materials since the Fermi level crosses a rather high peak of density of states, which is roughly 50% metal 50% boron–carbon in character (see Figure 9). The states below the Fermi level are highly localized on the boron and carbon atoms, while the ones above are mainly metallic. However, the metal and nonmetal states are not segregated but are mixed all along the energy scale. This mixing reflects the covalent character, which occurs between the metallic and boron–carbon layers. This is reflected too by an incomplete electron transfer from the metal atoms toward the boron and carbon ones (see the atomic net charges in Table 3). A total of roughly three π-electrons per B_2C unit is computed after interaction with the metal network, versus four before interaction.

Using a rigid band model, an examination of the data given in Table 3 indicates that the B–C and B–B overlap populations vary in the opposite way when electrons are added. The same result was observed for the two-dimensional layers. The role of the metal atoms is in turn to weaken the B–B bonds and to enhance the B–C ones. Interaction between the metal and nonmetal frameworks leads to some depopulation of states which are B–B bonding and B–C antibonding. Consequently, the B–B and B–C bond strengths are weaker and stronger, respectively, than they were before interaction with the metal network (compare Tables 2 and 3).

According to the values given in Table 3, the metal–metal interactions in ThB_2C and α-UB_2C are slightly bonding in the layers but slightly antibonding between layers. They are hardly perturbed upon the addition of electrons. These metal–metal contacts derive mainly from through-bond interactions due to some mixing of metal–metal bonding orbitals in occupied orbitals of the B_2C network. Although, the metal–metal separations measured in ThB_2C or α-UB_2C are comparable to that observed in metallic elements, they are not so strong. Indeed, in the title compounds the metal atoms are in a high oxidation state and therefore much more contracted than in the metallic elements.[27]

Electronic Structure of YB_2C

We will use the same approach to explore the third compound of the series MB_2C, namely YB_2C.

(a) The 2-D Net of Boron and Carbon. Assuming first a pure bonding scheme between the metal atoms and the B_2C sublattice, we end up without ambiguity with the Y^{3+}, $[B_2C]^{3-}$ formal charges. For this electron count, four mesomeric Lewis formulas satisfying the octet rule can be proposed, consistent with the partial double bond character of the B–C bonds (see Figure 3). One is shown in **5**. Note that, as well as in the $[B_2C]^{4-}$ subunit **2**, the boron and carbon atoms of **5** follow the octet rule and provide four π-electrons per $[B_2C]^{3-}$ subunit.

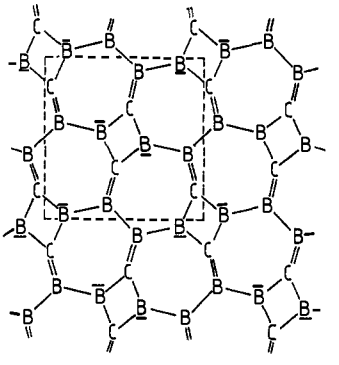

5

The band structure, density of states (DOS), and COOP curves of the 2-D B_2C net of YB_2C are shown in Figures 10 and 8c. Population analysis data, total electronic energy, and Fermi levels for several electron counts are collected in Table 2. It is remarkable that the results corresponding to a $[B_2C]^{3-}$ charge are very similar to those obtained for the $[B_2C]^{4-}$ 2-D nets of ThB_2C and α-UB_2C, in particular the number of π-electrons (4.00), the semimetallic character of the hypothetical 2-D net, and the change of sign of the B–B COOP curve at the Fermi level. These similarities give us some confidence in attributing a formal oxidation state of 4+ to the metal atoms in ThB_2C and α-UB_2C.

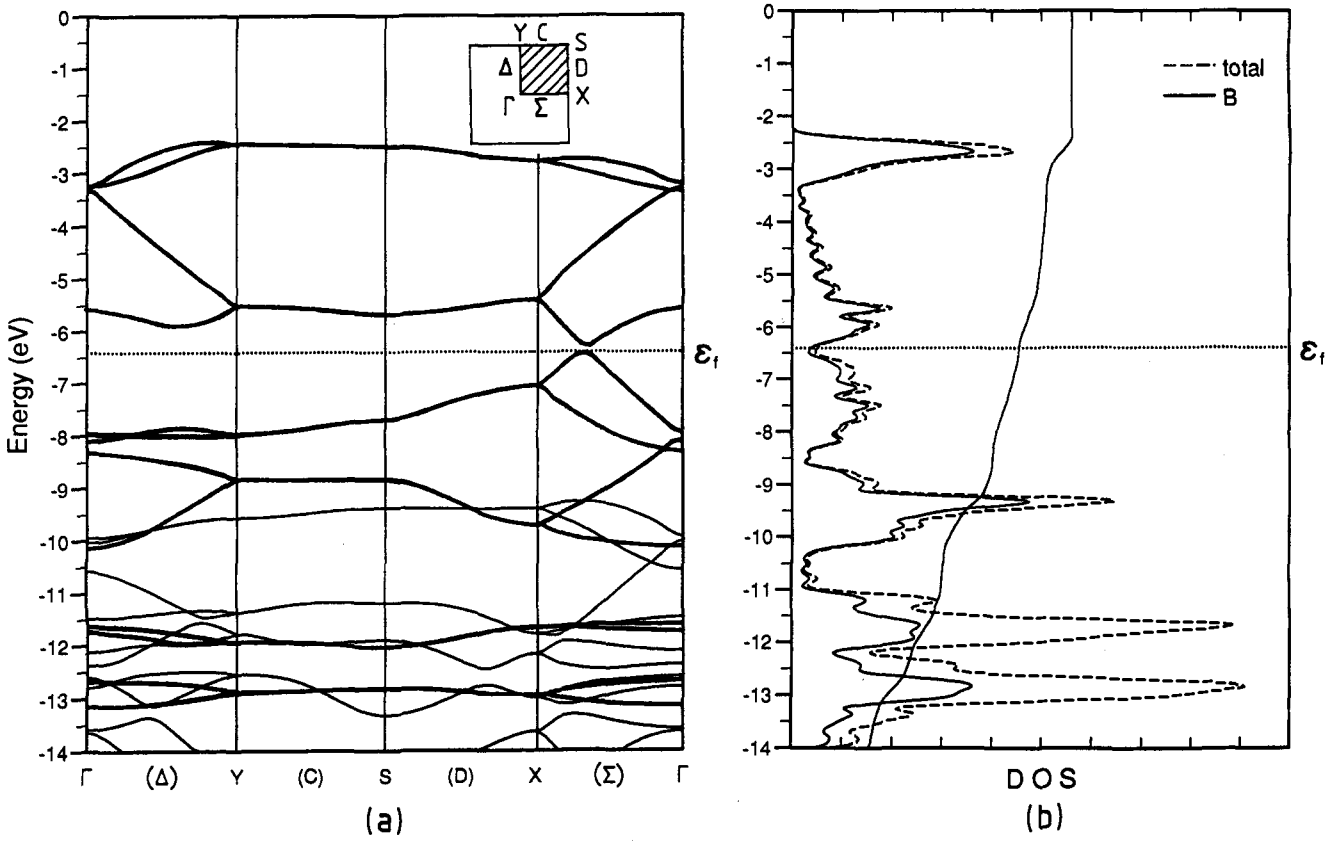

Figure 10. (a) Band structure and (b) total density of states (dashed line) and boron contribution (solid line) for the 2-D boron–carbon net encountered in YB_2C. The Fermi level is indicated for a charge of 3- per B_2C unit. π-bands are in bold line.

Table 3. Characteristics Computed with Different Valence Electron Counts for the 3-D ThB_2C, α-UB_2C, and YB_2C Materials

	electron number[a]					
	13			14		
struct type	ThB_2C	α-UB_2C	YB_2C	ThB_2C	α-UB_2C	YB_2C
Re (eV)[b]	0.00	−0.21	0.33	0.00	−0.20	0.46
ϵ_F (eV)[c]	−9.23	−9.28	−9.27	−8.44	−8.39	−8.18
	Overlap Populations[d]					
B–B	0.668	0.689	0.752	0.723	0.774	0.773
B–C	1.025	0.956	0.753	0.971	0.893	0.748
M–B	0.078	0.087	0.125	0.081	0.088	0.134
M–C	0.161	0.193	0.141	0.166	0.203	0.126
M–M (intra[e])	0.044	0.043	0.080	0.051	0.046	0.106
M–M (inter[e])	−0.001	−0.012	−0.028	0.005	−0.016	−0.028
	Atomic Net Charges					
B	0.06	0.10	0.10	−0.12	−0.15	−0.05
C	−1.21	−1.22	−1.10	−1.39	−1.43	−1.21
M	1.09	1.02	0.90	1.63	1.73	1.31

[a] Per MB_2C unit. [b] Relative energy for a given electron count. [c] Fermi level. [d] Averaged. [e] Intra: intralayer, inter: interlayer.

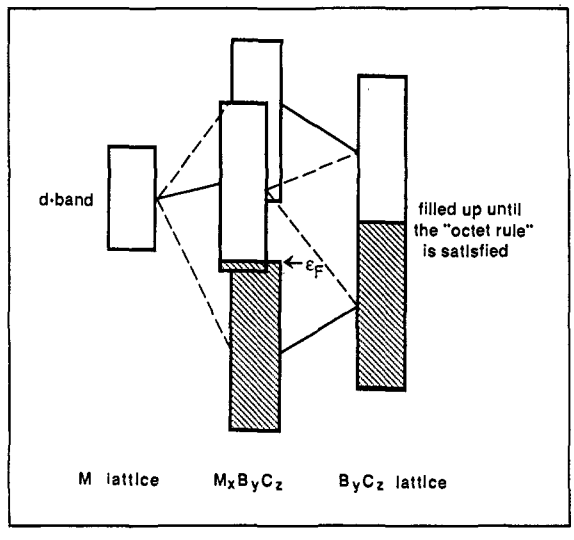

Figure 11. Simplified interaction diagram of MB_2C rare-earth boro-carbide compounds.

A comparison of the different B–C layers tells us that the latter arrangement, observed in YB_2C, is unlikely to be encountered with metal elements possessing four valence electrons. Extra electrons would in turn populate B–B *and* B–C antibonding levels, destabilizing significantly the two-dimensional arrangement (see Table 2 and Figure 8c).

(b) The Full YB_2C Structure. The role of the metal in YB_2C can be traced in the DOS represented in Figure 9c. Some computed data are collected in Table 3 and compared to the corresponding ones obtained for ThB_2C and α-UB_2C. The general conclusions drawn for the latter structures are valid again for YB_2C. The Fermi level cuts a high peak of density of states; the material should be then metallic. The metal contribution in the boron–carbon valence band is rather important. As found for ThB_2C and α-UB_2C, this covalent interaction leads to a weakening and a reinforcing of the B–B and B–C bonds, respectively. The electron transfer from the metal atoms toward the nonmetal net is not complete (see Table 3). Again, the number of π-electrons per B_2C unit is now nearly three, instead of four before interaction with the metal network, reflecting important donation from the $[B_2C]^{3-}$ layers into the Y^{3+} sheets.

General Discussion and Concluding Remarks

The present study allows us to understand the reasons why the B_2C 2-D nets encountered in ThB_2C and α-UB_2C are structurally related and why the arrangement of the B_2C net observed in YB_2C is different. This is indeed related to the formal oxidation state of the metal atoms (4+ for Th and U and 3+ for Y) and therefore to the electron count of the B_2C sublattice. Despite this difference, all the B_2C sublattices present the same number

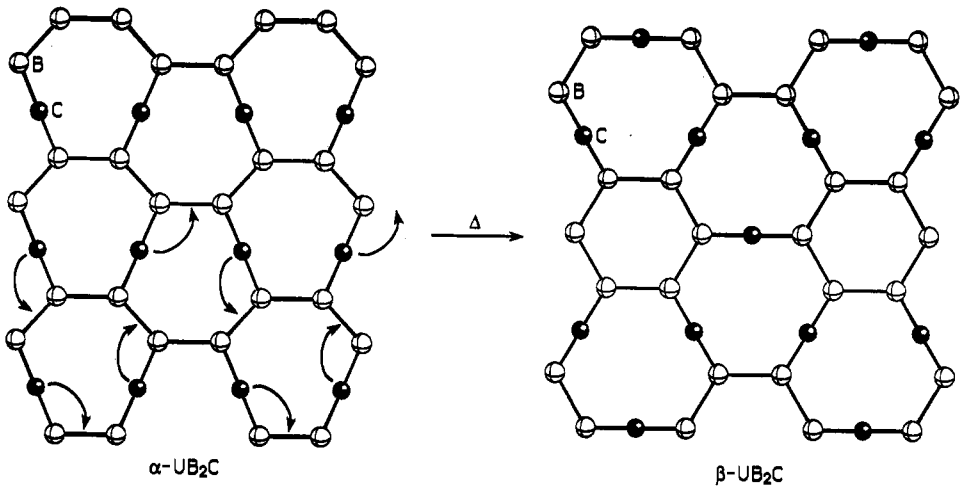

Figure 12. Hypothetical concerted mechanism for the α-UB_2C to β-UB_2C (ThB_2C-type) reaction.

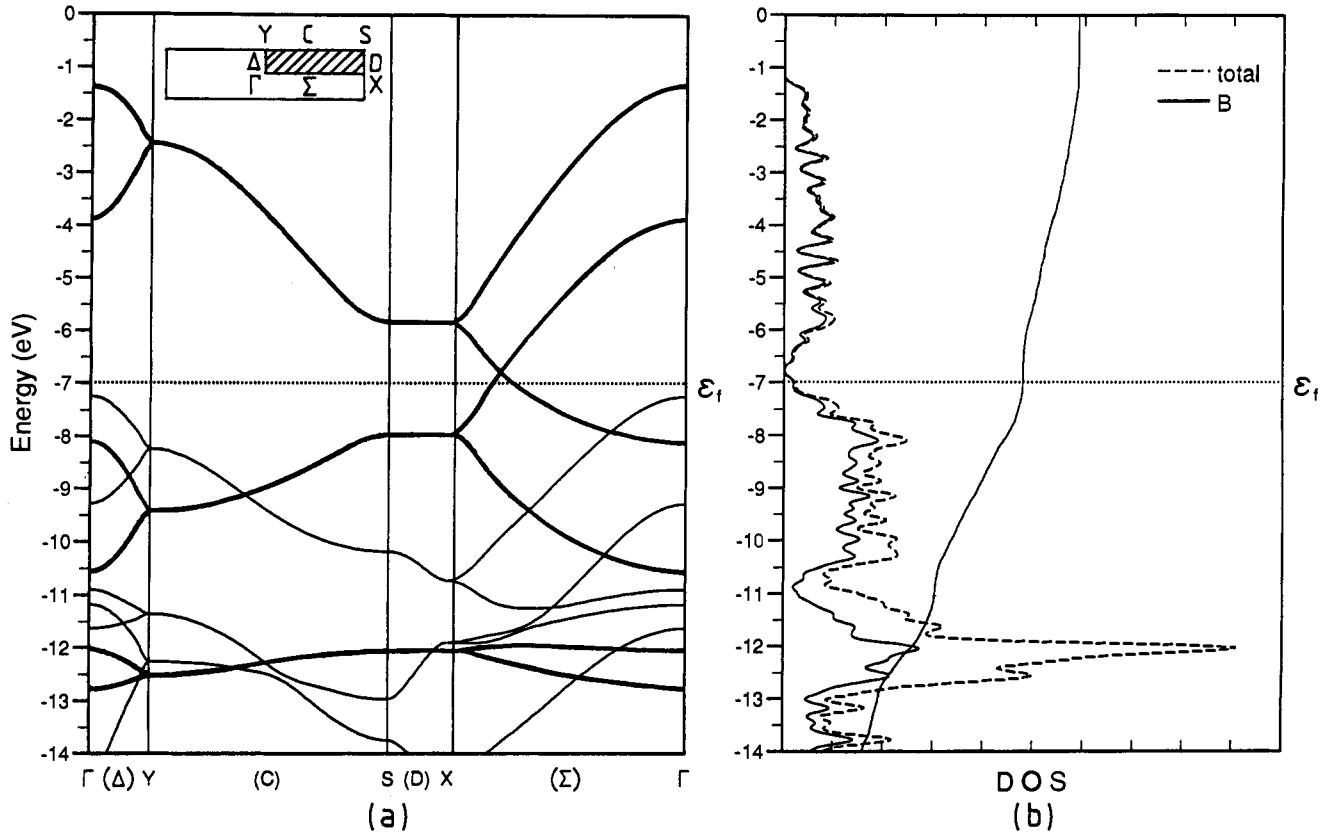

Figure 13. (a) Band structure and (b) total density of states (dashed line) and boron contribution (solid line) for the 2-D boron–carbon net **6**. The Fermi level is indicated for a charge of 4– per B_2C unit. π-bands are in bold line.

of π-electrons and interact in a similar way with the metallic framework, i.e., through electron donation. In some way, the interaction between the metallic and light-atom sublattices is related to the bonding between metal and ligands in high oxidation state transition-metal complexes. Since in any case the d-band of the metallic sublattice is empty, the metal–metal bonding present in those materials, results mainly from through-bond interactions, via mixing of metal–metal bonding orbitals in the occupied orbitals of the B_2C sublattice. This general situation is schematized in Figure 11.

It has been previously shown by one of us that the α-UB_2C phase rearranges in the ThB_2C structure-type at high temperature to give the β-UB_2C phase.[7] From the comparison of the two arrangements, a possible isomerization reaction via the concerted mechanism shown in Figure 12, was proposed. From experimental observations, the phase transition is nonmartensitic but diffusion controlled with a transformation enthalpy of roughly 1 KJ per mole of UB_2C. Considering that the atomic diffusion path occurs only inside the organic layers, we have tentatively evaluated the energy of a hypothetical transition state, the structure of which being the midpoint of the coordinate of the considered reaction shown in Figure 12. Though the process is symmetry allowed, the calculated value for the activation energy is high (*ca.* 6 eV per $[B_2C]^{4-}$ unit). The reason lies in the fact that the connectivity between some atoms at the transition state is much too high for the considered electron count, so that antibonding states are occupied. We thus suggest that, if the two-dimensional character of the nonmetal sublattice is maintained during the transition process, the metal sublattice may act as an electron buffer, helping the α-$UB_2C \leftrightarrow \beta$-$UB_2C$ phase transformation by first accepting and then releasing electrons during the transit: either by using its d-band or even its f-orbitals. Indeed, there is no reason to rule out the possibility of a 3+ oxidation state ($5f^3 6d^0$) for the uranium atoms near the transition state, since it is rather commonly

observed in chemistry.[27] Because of its low symmetry, it was not possible to guess with enough confidence the structure of a hypothetical 3-D transition state. Therefore, we have checked the electron-accepting capability of the metal d-band on a MB_2C half-sandwich slab made of one sheet of nonmetal atoms described above and one hexagonal sheet of metal atoms. The presence of the metal atoms lowers the activation energy to *ca.* 3 eV, due to bonding M–M d states which act as electron sinks. Owing to the various approximations we made (especially in maintaining the nonmetal net strictly planar), this result appears to be rather satisfactory.

At this point of the discussion, it is noteworthy mentioning that the 2-D B_2C nets observed in ThB_2C and α-UB_2C are not the only ways to arrange basic building blocks of type **1**. An alternative arrangement would be to have boron zigzag chains linked to each other by sp carbon atoms, as depicted in **6**. Note that a related boron–carbon net based on the assemblage of linear BCBCB units is observed in $Gd_2B_3C_2$.[8] A parallel with the configurational problem of polyacetylene can be drawn here. In fact, among the different ways to arrange sp^2 CH groups together, the simplest are to form finite cyclic entities such as benzene C_6H_6 or one-dimensional chains such as *all-trans*- and *cis/trans*-polyacetylene.[23b,36] The geometrical disposition of the boron atoms in the light-atom layers presented here (ThB_2C, α-UB_2C, **6**) are reminiscent of that of carbon atoms in $(CH)_x$ oligomers. In ThB_2C, the boron atoms form hexagons like in benzene, linked to each other via sp carbon atoms. The boron backbone in α-UB_2C can be seen as *cis/trans*-polyacetylene-like chains tethered to each other again with sp carbon atoms. Finally, the layer proposed in **6** results from the association of boron *all-trans*-polyacetylene-like chains through sp carbon atoms.

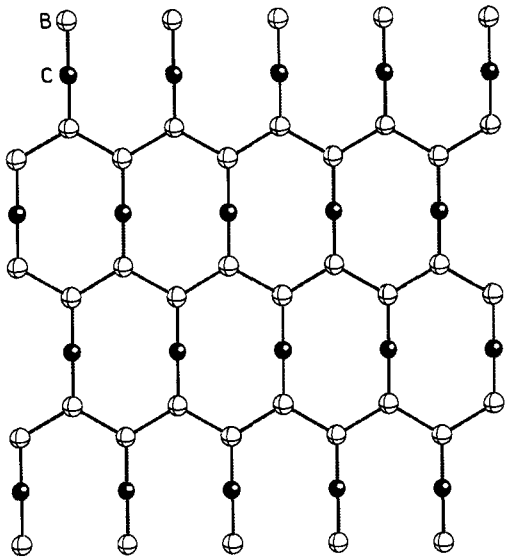

6

The results of our calculations on the hypothetical $[B_2C]^{4-}$ layer **6** are given in Table 2. They are overall similar to that of the corresponding nets of ThB_2C and α-UB_2C. The band structure and the DOS curves (shown in Figure 13) and the COOP curves (not shown here) are almost identical to the ones computed for the net present in α-UB_2C. This is not too surprising since *all-trans*- and *cis/trans*-polyacetylenes are also highly comparable.[23b,36] Therefore, we propose that such a 2-D $[B_2C]^{4-}$ sublattice (or an isoelectronic system) could exist as a part of a metal ternary compound.

As in the case of the $[B_2C]^{4-}$ 2-D nets encountered in ThB_2C and α-UB_2C, the band structure given in Figure 13a indicates a semimetallic situation for the hypothetical 2-D net **6**. This deserves explanation. The similarities between the three nonmetal nets can be understood by first comparing the π electronic structure of the following intermediate building blocks in which B–B bonding is present: a hexagonal $[BCB]_6^{24-}$ molecular fragment (**7**) for ThB_2C, and, for example, an *all-trans* 1-D chain made of $[B_2C]^{4-}$ units (**8**) present in **6**. In these models, B–B π interactions can be described by the simple diagram shown in Figure 14. Each of the three π orbitals of the repeat unit $[B_2C]^{4-}$ generates a band in the 1-D chain or a group of six levels in the cyclic fragment. The band (or block of six levels) generated by π_1 is narrow, due to its small coefficient on boron atoms. This is not the case for the bands derived from π_2 and π_3, which are much more dispersed. It turns out that the top of the π_2 band (or block), which is the HOMO of the system, is situated roughly 0.5 eV below the bottom of the π_3 band (or block), which is the LUMO. Of course, a similar conclusion can be drawn for a 1-D *cis/trans* chain of $[B_2C]^{4-}$ present in α-UB_2C. In the real nonmetal 2-D nets of ThB_2C, α-UB_2C and **6**, supplementary through bond B···B interactions are present, leading to an increase of the band dispersion. Consequently, the π_2 and π_3 bands nearly or slightly overlap so that the HOMO/LUMO gap vanishes. Clearly, this semimetallic situation is the result of both the *topology* of the nets and the *electronegativity difference* between boron and carbon.

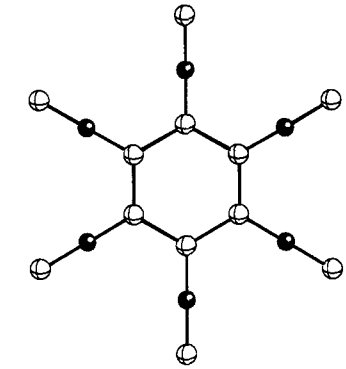

7

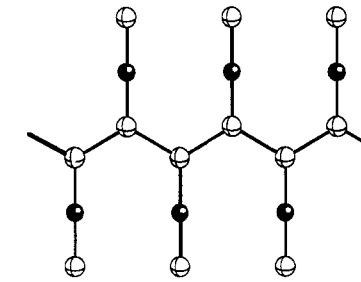

8

Since the π_2 and π_3 orbitals of the $[B_2C]^{4-}$ repeat unit are both primarily boron-localized and relatively close to each other in energy, they mix significantly in **7** and **8**. Such a phenomenon can be viewed as a second-order interaction between the π_2 and π_3 bands (or group of six levels). As a result, the top of the π_2 band loses most of its B–B antibonding character, by losing most of its localization on the boron chain. On the other hand, the bottom of the π_3 band loses most of its B–B bonding character, by losing most of its localization on the boron chain. This is illustrated in Figure 14, where the HOMO and LUMO of **7** and **8** are depicted. In the nonmetal 2-D nets of ThB_2C, α-UB_2C, and **6**, supplementary mixing between the π_2 and π_3 bands occurs, transforming the weakly antibonding character of the upper part of the π_2 band into a bonding one. Similarly, the lower part of the π_3 band becomes antibonding. This explains why the sign of the B–B overlap population changes, not twice (at the middle of the π_2 and π_3 bands) as expected if there was no mixing, but once (near the Fermi level, where the two bands touch each other).

We turn now the discussion to the possibility of the B–B bond alternation in the 2-D nets of ThB_2C, α-UB_2C, and **6**. Indeed,

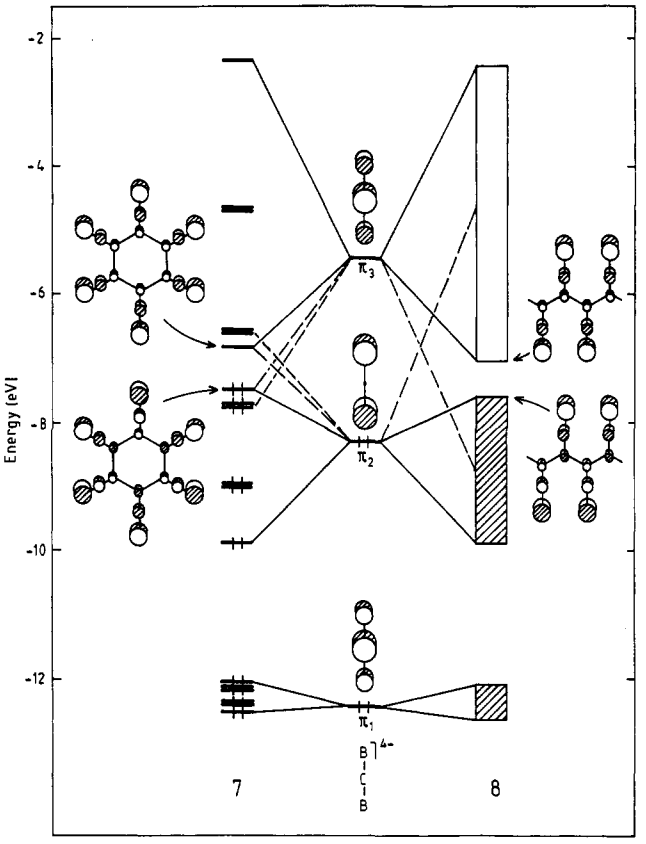

Figure 14. Generation of the π interactions in the molecular fragment $[BCB]_6^{24-}$ (**7**) and the *all-trans* 1-D $[B_2C]^{4-}$ chain (**8**) from the π orbitals of the $[B_2C]^{4-}$ unit.

we know that sometimes X-ray diffraction can fail to observe alternating long and short B–B contacts.[10,11] Such a distortion would suggest a Lewis structure like **9** for the $[B_2C]^{4-}$ entities encountered in the different nets. Since there is no HOMO/

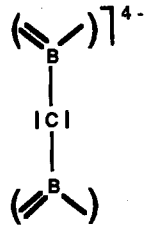

9

LUMO degeneracy in the models **7** and **8** (see Figure 14), only a second-order Jahn–Teller or Peierls instability could account for B–B bond alternation in these models. Although the HOMO/LUMO gaps are small, the levels which are involved have a poor localization on the B–B bonds and consequently do not favor the distorted structure. The preference for regular chains (or rings) of boron atoms is expected to be even larger in the 2-D nets and the real 3-D MB_2C structures.

Finally, the similarity of the 2-D net of the $[B_2C]^{3-}$ of YB_2C with the other $[B_2C]^{4-}$ 2-D nets (DOS and COOP curves) can be understood in the same way. This peculiar arrangement presents finite (but already rather long) chains of four sp^2 boron atoms linked together through carbon atoms. Therefore, the π electronic structure of this net is strongly related to that of the other nets. On the other hand, the σ electronic structure is different. Since the carbon atoms are this time three-connected, they do not hold a σ long pair, accounting for the lowest charge of the B_2C repeat unit.

Acknowledgment. Thanks are expressed to L. Hubert for the illustrations. F.W. is grateful to the Région Bretagne for financial support. P.R. is grateful to the Austrian Academy of Sciences for a research grant at the INSA, Rennes, France.

Appendix

All molecular and tight-bonding calculations were carried out within the extended Hückel formalism[23] using standard atomic parameters for B and C. Different sets of parameters for the metal atoms were used. They basically led to the same qualitative conclusions, whatever metal was considered. Therefore, in order to facilitate the comparison between the different materials, we chose to present here the results obtained with the parameters of yttrium. The role of the rather contracted f orbitals for Th and U has been neglected, and thus they were not included in the calculations. The exponent (ζ) and the valence shell ionization potential (H_{ii} in eV) were, respectively, 1.3, −15.2 for B 2s; 1.3, −8.5 for B 2p; 1.625, −21.4 for C 2s; 1.625, −11.4 for C 2p; 1.39, −8.6 for Y 5s; 1.39, −5.0 for Y 5p. The H_{ii} for Y 4d was set equal to −8.4 eV. A linear combination of two Slater-type orbitals of exponents $\zeta_1 = 4.33$ and $\zeta_2 = 1.4$ with weighting coefficients $c_1 = 0.5827$ and $c_2 = 0.6772$ was used to represent the 4d atomic orbitals of Y.

The experimental structures of ThB_2C,[6] α-UB_2C,[7] and YB_2C[5] were used for the calculations. In models **6**, **7**, and **8**, B–B and B–C distances comparable to that observed in ThB_2C and α-UB_2C were used. Angles of 120° were taken around the boron atoms.

For the calculations of the density of states, overlap populations and atomic net charges of the 3-D materials, sets of 28, 35, and 24 k points, were chosen in the irreducible wedge of the appropriate Brillouin zone of the ThB_2C, α-UB_2C, and YB_2C structure types, respectively. The 28, 35, 28 and 48 k points, taken in the part of the Brillouin zone, were used for the DOS calculations on the 2-D organic networks present in ThB_2C, α-UB_2C, YB_2C, and **7**. All k point sets were chosen in accordance with the geometrical method described by Ramirez and Böhm.[37]